Supplemental Information:

Polymeric nanocarriers co-encapsulating PET probes and protein therapeutics

Chester E. Markwalter[1a], Leon Z. Wang[1], Ola M Sharaf[2], Prashanth Padakanti[2], Mark Esposito[3], Brian K. Wilson[1], Eric Blankemeyer[2], Sean D. Carlin[2], Abass Alavi[2], Robert K. Prud'homme[1]*

1) Optimization of Surface Properties

To determine the relative effects of crosslinker, hydrophobic block size, and polymer type, a range of formulations were prepared using standard iFNP techniques. The PEG coating was carried out in a CIJ mixer with deionized water as an antisolvent. The PEG-containing block copolymer corresponded to the inverse NC polymer selection ($PS_{1.6k}$-*b*-PEG_{5k} or PLA_{5k}-*b*-PEG_{5k} for non-degradable or degradable formulations, respectively). The zeta potentials were then measured in 0.1x PBS (15mM sodium phosphate and sodium chloride). The results are tabulated in Table S1. For the PS-based formulations, negatively charged iFNP-NCs were associated with much larger hydrodynamic diameters as measured by dynamic light scattering (DLS), despite initial sizes that were similar. Iron-crosslinked NCs were around 153 nm, on average, while iFNP-NCs with negative zeta potentials averaged 273 nm after coating.

Table S1: Zeta potentials (ζ, mV) for different iFNP-NC formulations. Ammonia was added, where noted, after inverse NC assembly to promote ionic interactions by neutralizing the pH of the core.

Biologic	Water (vol%)[a]	Hydrophobic Shell[b]	Crosslinker	ζ (mV)
20kDa Dex	5%	52kDa PS	Ca/NH_3	-39
Lysozyme	5%	5kDa PS	Zn/NH_3	-35
Lysozyme	5%	5kDa PS	Ca/NH_3	-32
3kDa Dex	10%	5kDa PS	TEPA	-32
3kDa Dex	5%	5kDa PS	TEPA	-31
20kDa Dex	10%	5kDa PS	TEPA	-29
Lysozyme	5%	5kDa PS	TEPA	-27
Lysozyme	5%	52kDa PS	Fe	-3.4
3kDa Dex	5%	5kDa PS	Fe	-3.3
20kDa Dex	10%	5kDa PS	Fe*	-3.2
20kDa Dex	10%	5kDa PS	Fe/NH_3	-3.0

Lysozyme	5%	5kDa PS	Fe	-2.0
Lysozyme	5%	15kDa PS	Fe	-0.6
20kDa Dex	10%	5kDa PLA	Ca/NH_3	-4.6
Lysozyme	5%	5kDa PLA	TEPA	-4.2
Lysozyme	5%	20kDa PLA	TEPA	-3.6
20kDa Dex	10%	20kDa PLA	TEPA	-2.9
20kDa Dex	10%	20kDa PLA	Ca/NH_3	-2.7
5kDa Dex	10%	20kDa PLA	Ca/NH_3	-2.3

*[a]Water content in the DMSO stream used to form the inverse NPs. Water promotes crosslinking but we had hypothesized that too much water would lead to an incomplete hydrophobic shell. This was not proven by the data. [b]Block size used in the inverse NC formation process with the full stabilizer described in the main text. *Iron was added after inverse NC assembly for this formulation rather than during mixing in the CIJ.*

We also assessed whether changing the mass ratio of PEG stabilizer influenced the measured zeta potential (Figure S1). While there was a slight trend towards less negative values, we hypothesize that this may reflect a growing population of PS-*b*-PEG micelles that were biasing the measurement. We found zeta potentials became 38% more neutral on average when the crosslinking time for the inverse NCs was increased from 30 minutes to 18 hours at 2-8 ºC. We posit that this reflects a secondary, slow relaxation/rearrangement regime after the initial complexation, leading to a more stable state for the hydrogel. We implemented this age time for formulations used during *in vivo* testing.

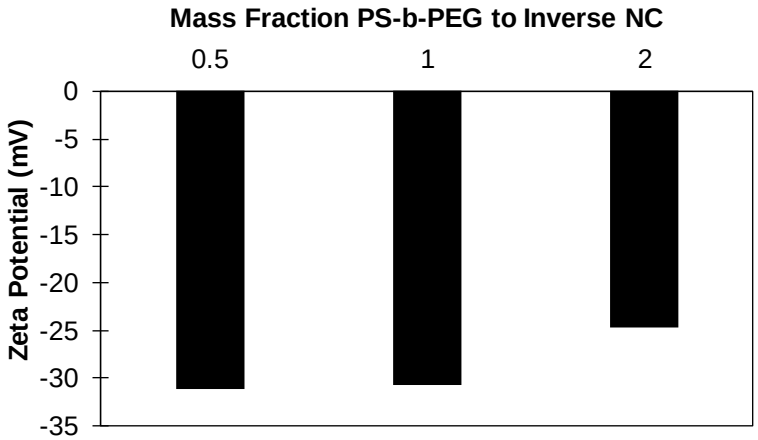

Figure S1: Average zeta potential of dextran iFNP-NCs formed by calcium/ammonia crosslinking of PS_{5k}-b-PAA_{5k}. The $PS_{1.6k}$-b-PEG_{5k} ratio was varied four-fold but found to have a weak influence on the measured value. It is possible that the formation of neutral micelles of $PS_{1.6k}$-b-PEG_{5k} led to the slight

decrease in zeta potential seen at the 2:1 ratio while a negative population containing the iFNP-NC remained.

2) Buffer stability findings

Zeta potential screening at 16 hours incubation time identified a buffer effect as well as a molecular weight effect for PS-iFNP-NCs that was very mild for PLA-iFNP-NCs.

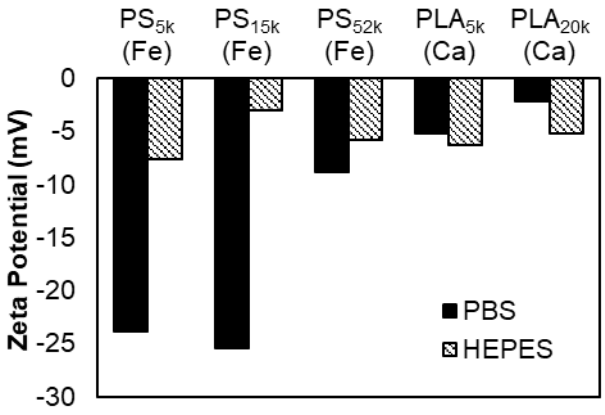

Figure S2: Zeta potential of iFNP-NCs after 16 hours incubation in PBS (solid bars) and HEPES buffer (hashed bars) at 37ºC. The naming convention lists the hydrophobic block molecular weight used in assembling the inverse NC with the crosslinker given in parentheses.

The kinetics of zeta potential changes in buffer were monitored to determine how quickly the negative zeta potential developed for PS-iFNP-NCs. A formulation using $PAA_{4.8k}$-*b*-PS_{5k} with iron crosslinking was employed for the test. Phosphate buffered saline (PBS, pH 7.5, 160mM) and HEPES buffer at the same osmolarity were used. The HEPES buffer was prepared at two pH values to determine whether the counterion or pH had a stronger effect. As seen in Figure S3, both parameters influenced the zeta potential changes over time but PBS had strong and immediate effects. The pH changes likely indicate increasing tendency to form iron oxide-hydroxide species. By DLS, the HEPES samples were unchanged while the PBS sample had grown over 100 nm relative to the input.

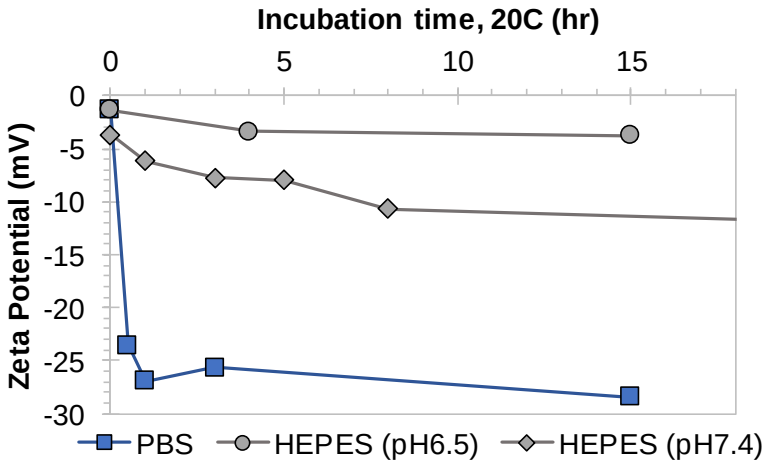

Figure S3: Kinetics of buffer stability for iFNP-NCs formed using a 5 kDa PS block and iron crosslinking for the inverse NP assembly. The rapid failure in PBS is not recapitulated in HEPES, where a slight pH effect is observable. This suggests that a combination of factors is influencing the stability of the iron crosslinks: a specific effect from phosphate as well as a general pH dependency.

We conducted a longer kinetic study in HEPES with iFNP-NCs formed using the PAA_{5k}-*b*-PS_{52k} block copolymer, PLA_{15k}-*b*-$PAsp_{2k}$ (called Gen2-PLA below), or $PAsp_{5k}$-*b*-PLA_{x}-*b*-$PAsp_{5k}$ (called PLA_{xk} below). The coated NCs were incubated at 37°C and assayed for size (Figure S4). As expected, the PLA_{15k}-*b*-$PAsp_{2k}$ exhibited the best stability of the PLA formulations.

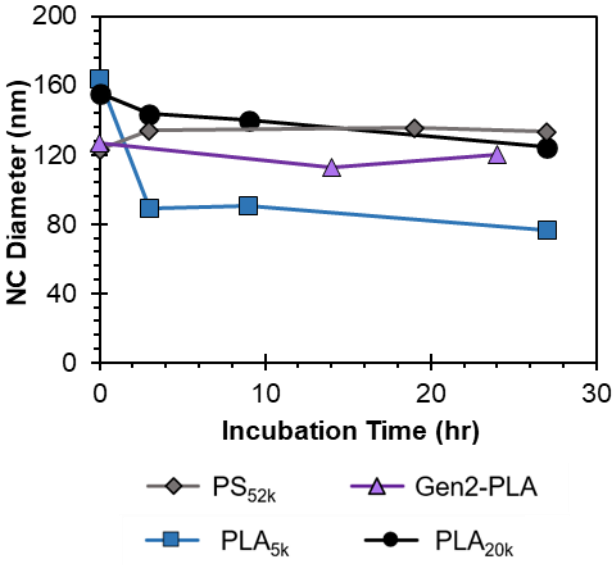

Figure S4: NC size changes for the best-performing formulations, in HEPES buffer at 37 ºC. Inverse NCs were stabilized using a block copolymer containing PLA_{5k} (blue square), PLA_{20k} (black circle), PS_{52k} (grey diamond), or a generation 2 polymer, $PAsp_{2k}$-b-PLA_{15k} (purple triangles). PLA formulations were calcium crosslinked. The PS formulation used iron.

3) Co-encapsulation of ‘762 with iFNP-NCs

To separate co-encapsulated ‘762 from ‘762 sequestered into micelles, we validated a size exclusion chromatography method to separate the two populations, as shown in Figure S5. We compared PLA and PS formulations and then evaluated the effect of PS-*b*-PEG ratio on co-encapsulation using the PS-iFNP-NC formulation.

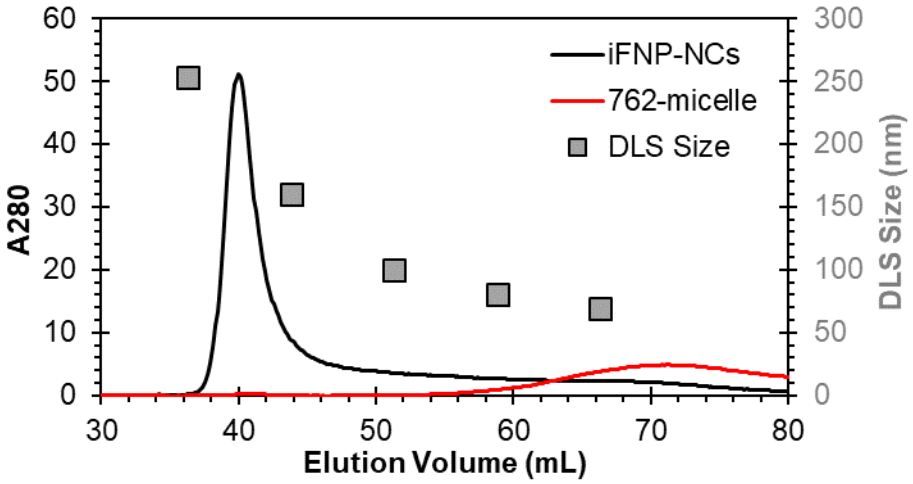

Figure S5: Characterization of S-500 SEC packing using iFNP-NC (black) and micelle (red) formulations demonstrating good separation between the two fractions. SEC traces are the absorbance at 280 nm as a function of elution volume. The average DLS size in each fraction is shown by the gray squares. Prior to injection, the iFNP-NCs were measured by DLS to be 150nm and the control containing just ‘762 and PS-b-PEG were 66 nm.

The initial formulation employed the CIJ but found that increasing PEG block copolymer amounts resulted in increased micelle formation.

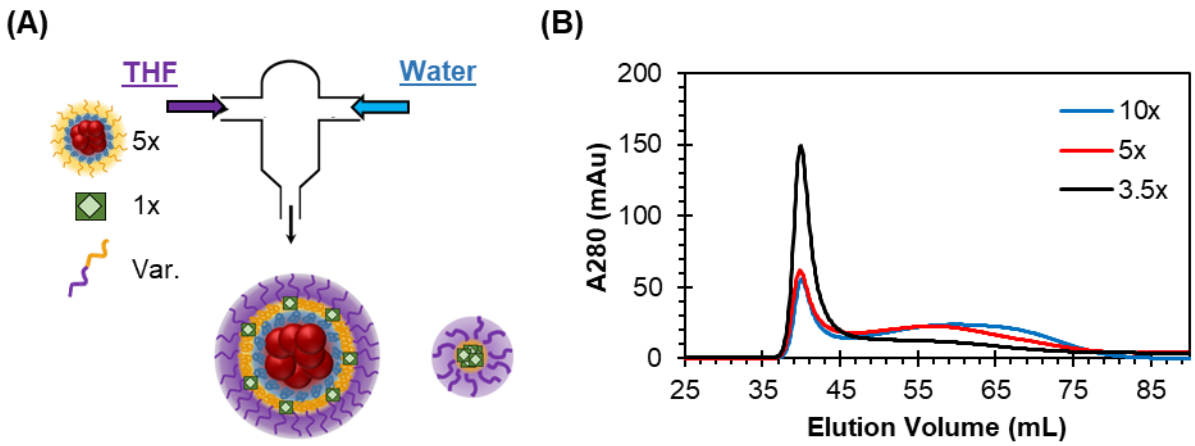

Figure S6: (A) Initial formulation for the co-encapsulation of '762 with inverse NCs in a CIJ mixer. All mass concentrations were scaled relative to the '762 input. (B) SEC traces for PS-iFNP-NCs with different ratios of PS-b-PEG used during coating, rescaled to a constant area under the curve to account for different injection concentrations. The mass ratios are as defined in (A). A clear shift towards smaller NC populations is evidenced through the increased signal after 60 mL elution. DLS analysis of the three samples indicated sizes of 152 nm (3x ratio), 125 nm (5x ratio), and 125 nm (10x ratio).

The same results were observed for PLA-iFNP-NCs.

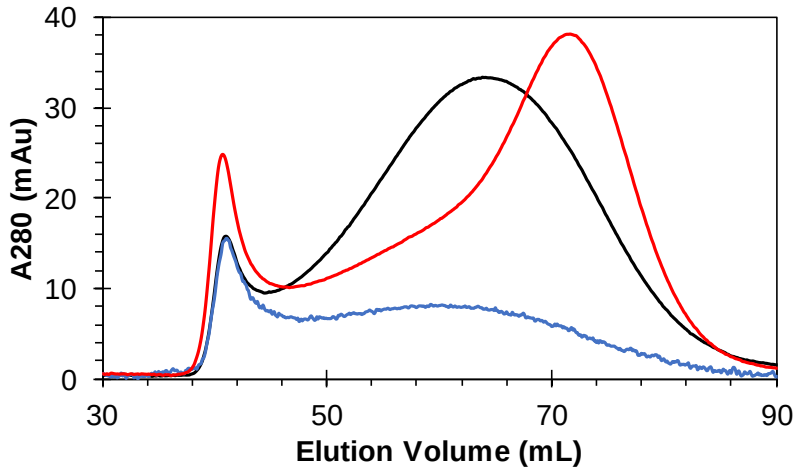

Figure S7: SEC analysis of PLA-iFNP-NCs produced with co-encapsulated '762 according to Figure S6-A. (Blue) iFNP-NCs without '762 addition, rescaled to match the trace (black) of iFNP-NCs with '762 included. Both formulations used a 0.75:1 ratio of PLA-b-PEG to iFNP mass. (Red) Replicate of the '762 with a 2:1 ratio of PLA-b-PEG indicating increased incorporation of '762 into micelles.

We modified the coating step to employ the MIVM and found that this permitted better coating of the iFNP-NCs without sequestering all '762 into micelles. The PS-iFNP-NC traces are shown in the manuscript and the PLA-iFNP-NC traces are below:

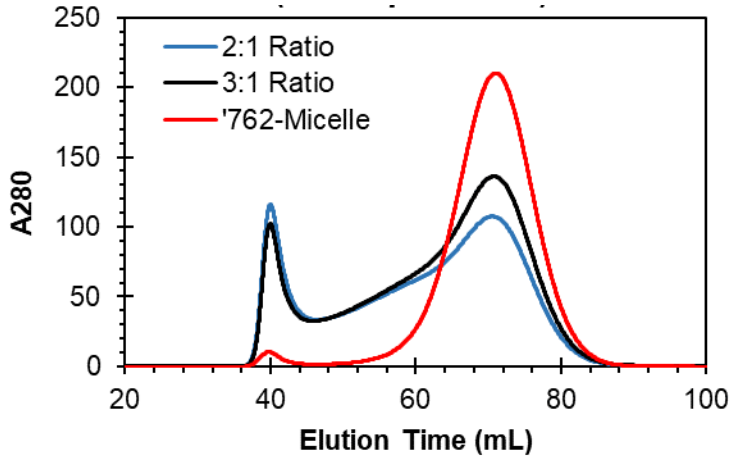

Figure S8: SEC traces for PLA-iFNP-NC formulations made using the MIVM. Before SEC fractionation, the DLS-measured size of the iFNP-NCs made at a 2:1 ratio of PEG:iFNP-NC was 114 nm. For the 3:1 ratio, it was 117 nm. The '762 micelles were 35 nm. After fractionation, the zeta potential of the iFNP-NC portion was -7mV (2:1 ratio) and -5.4 mV (3:1 ratio). The '762 micelles were -0.4 mV.

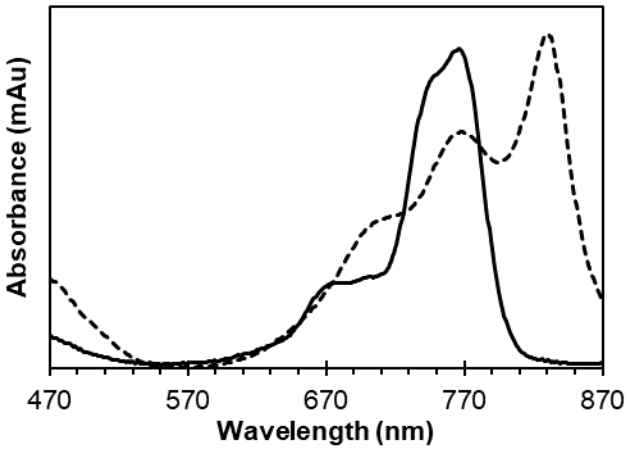

Figure S9: UV-VIS analysis of the PLA-iFNP-NC fraction after SEC (dashed line). The aggregation-induced peak at 830 nm is clearly visible but is lost upon dissolution in THF (solid line).

4) Hemolysis assay

The PLA-iFNP-NC (PEG) was produced using the Gen2-PLA formulation but lacked '762 to limit any assay interference. The FNP-NC (PEG) was produced using standard FNP conditions with a 11 kDa PLA core and $PLA_{4.2k}$-*b*-PEG_{5k} stabilizer at 50% mass and 30 mg/mL total mass concentration. FNP-NC (PAsp) was produced using $PAsp_{5k}$-b-PLA_{10k}-b-$PAsp_{5k}$ block copolymer as a negatively charged stabilizer. The negative control was sterile PBS and the positive control was 10 mg/mL Triton X-100. Blank samples were prepared using each formulation but the whole blood portion was replaced with PBS. No hemolysis was detected for any condition, with the

exception of the positive control (Figure S10). This indicates no adverse interactions with the red blood cell membrane.

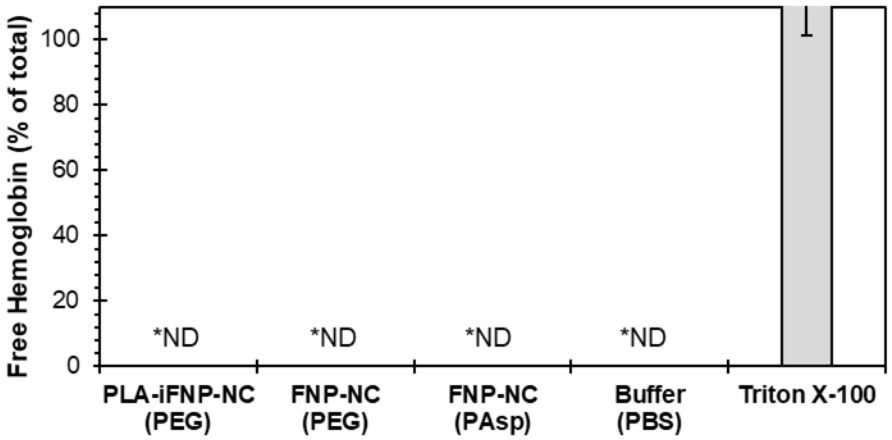

Figure S10: Hemolytic effects of NCs produced by FNP. The PLA-iFNP-NC (PEG) was produced using the Gen2-PLA but lacked '762 because this dye absorbance interfered with the assay. FNP-NC (PEG) was produced using standard FNP conditions using a 11 kDa PLA core and the standard PLA-b-PEG stabilizer. FNP-NC (PAsp) was produced using the ABA-10 block copolymer as a negatively charged stabilizer. The negative control was sterile PBS and the positive control was 10 mg/mL Triton X-100. No hemolytic activity was detected for any NC produced using these methods.

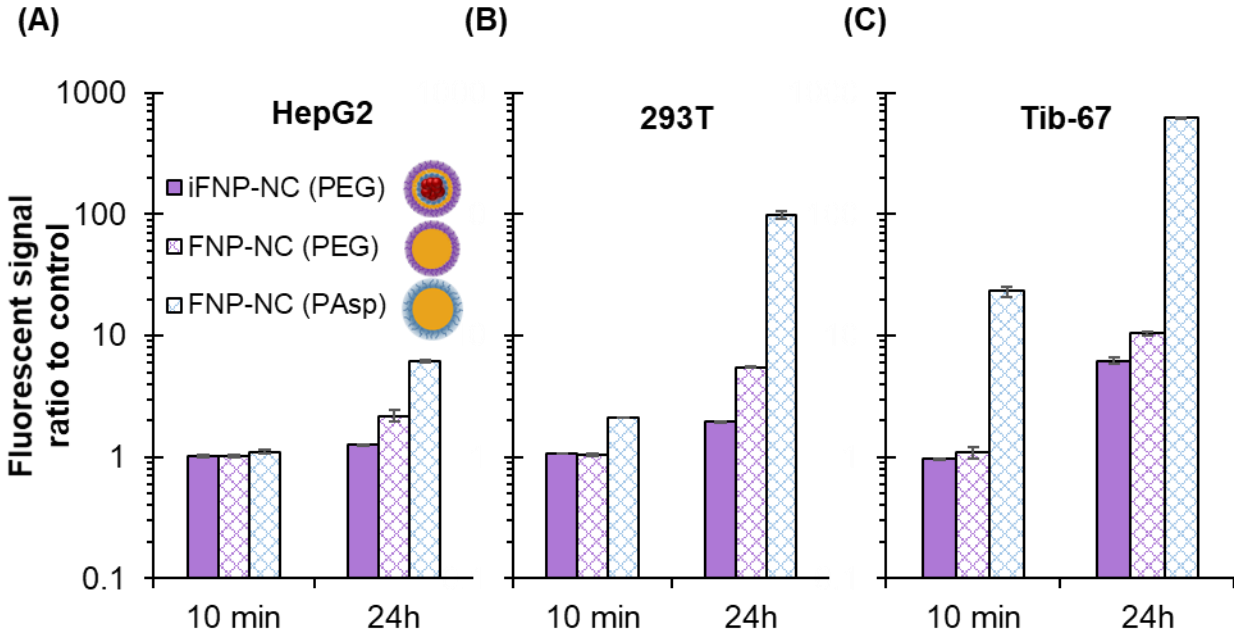

Figure S11: (A-C) Flow cytometry analysis of iFNP-NC and FNP-NC formulations incubated with the indicated cell line for 10 minutes and 24 hours. Mean fluorescence intensity was measured for each sample and reported as a ratio to the signal for DAPI staining only in the cell line. The bar represents the average of triplicates and error bars are the standard error. FNP-NCs were contained DiO and iFNP-NCs were AlexaFluor-488 labeled.

5) Copper Loading Validation

We next sought to confirm that ^{64}Cu was able to load into the PS-based iFNP-NCs, despite the glassy polymer state, and into PLA-based iFNP-NCs, despite phase separation of the dye. Successful chelation was then confirmed by a shift in absorbance maximum from 765 nm to 740 nm after redissolution in THF. This change was observed for both PS-iFNP-NCs (Figure S12) and PLA-iFNP-NCs (Figure S13). Crucially, the spectrum was unchanged by 24-hour incubation with a 10-fold excess EDTA. Robust loading performance was confirmed by incubation of three iFNP-NCs with radioactive ^{64}Cu. Unbound ^{64}Cu was detected in ultrafilter permeate after the reaction and indicated that >95% of radioactivity was bound to the NCs for all formulations (Figure S14).

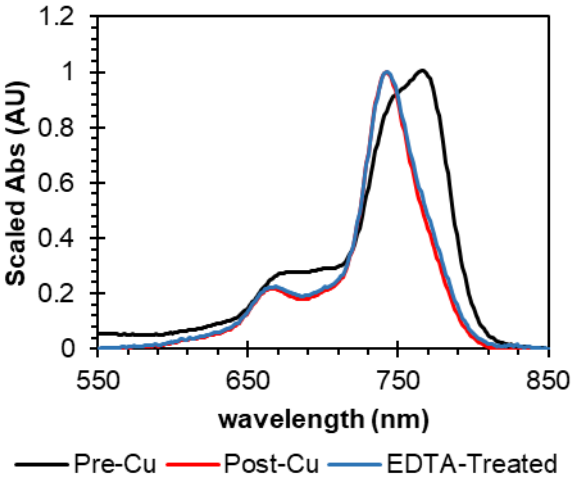

Figure S12: UV-VIS analysis of iFNP-NCs with co-encapsulated '762 (diluted in THF). Copper binding is indicated by a change in maximum from 762 to 740 nm. Bound copper was stable to EDTA exposure for 24 hours.

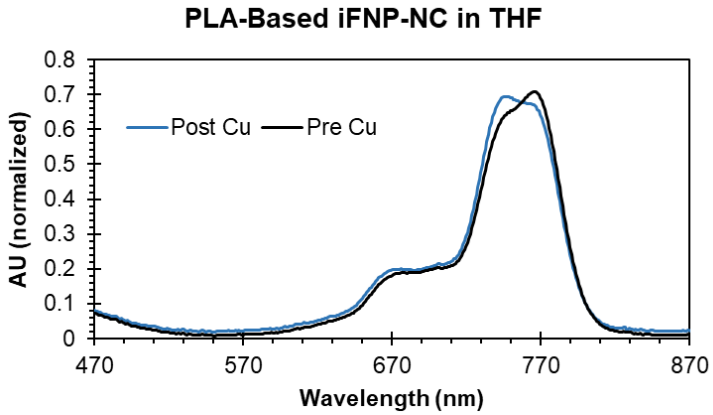

Figure S13: Analysis of PLA-iFNP-NC in THF before (black) and after (blue) copper incubation. The shift towards a peak at 740 nm indicates copper binding. No aggregation peak at 830 nm is observed because THF dissolves the dye from the stacked orientation.

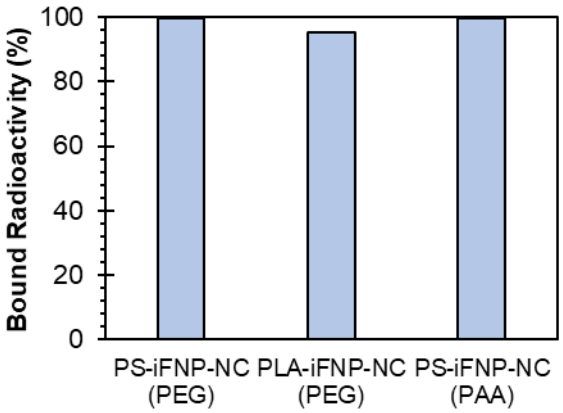

Figure S14: Activity measurements from 64Cu loading indicate minimal unbound 64Cu after 3 hours incubation at 37°C.

Table S2: DLS characterization of in vivo nanocarrier formulation size and zeta potential (ζ) with average values ± standard deviations.

	Size, nm	**ζ, mV**	**PDI**
PS-iFNP-NC	155±6	-5.5±2.1	0.13±0.01
PLA-iFNP-NC	120±7	-5.0±0.6	0.13±0.01

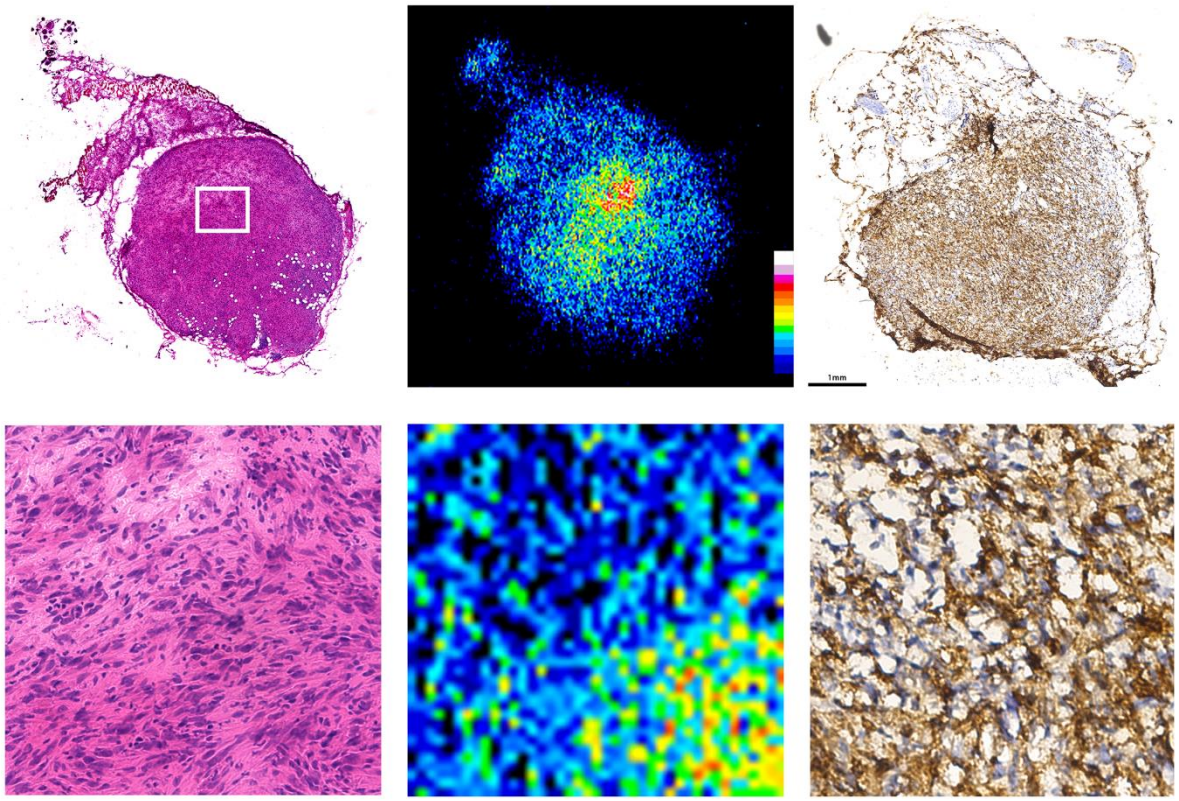

Figure S15: Spatially-registered tumor sections at low (top) and high (bottom) magnification from PS-iFNP-NC dosing. Left: tumor histology (H&E). Center: ^{64}Cu auto-radiography. Right: Immunohistochemistry for F4/80 mouse macrophage.